SANDIA REPORT

SAND96–2240 • UC–706
Unlimited Release
Printed February 1997

A JAS3D Material Model for Carbon Black-Filled Rubber

Robert S. Chambers

Prepared by
Sandia National Laboratories
Albuquerque, New Mexico 87185 and Livermore, California 94550
Sandia is a multiprogram laboratory operated by Sandia
tes
Corporation, a Lockheed Martin Company, for the United Sta
Department of Energy under Contract DE-AC04-94AL85000.

(See

Sandia National Laboratories

Issued by Sandia National Laboratories, operated for the United States Department of Energy by Sandia Corporation.

SAND96-2240
Unlimited Release
Printed February 1997

Distribution:
Category UC-706

A JAS3D Material Model for Carbon Black-Filled Rubber

Robert S. Chambers
Engineering Sciences Center
Sandia National Laboratories
Albuquerque, NM 87185

Abstract

Experimental work conducted by D. B. Adolf has shown that a separable K-BKZ constitutive equation works reasonable well in predicting the stress relaxation observed in single step strain experiments for carbon black filled rubber. However, the memory requirements and numerical efficiency of the K-BKZ equation do not make it well suited for use in a production, three-dimensional finite element code. As an alternative, D. J. Segalman, K. Zuo, and D. Parsons have developed a "damage-like" constitutive equation which is computationally attractive. This formalism has been installed in the JAS3D finite element code. The requisite code inputs and numerical details of the constitutive integration are discussed, and solutions to selected problems are presented. Comparisons are made to data collected from both single and double step strain experiments.

Acknowledgments

A special thanks goes to Dan Segalman for development of the proposed constitutive equations and for his endless patience and willingness to discuss material modeling issues. I also would like to thank Doug Adolf for his data and explanations of some of the peculiar behavior of carbon black-filled rubber. In addition, I want to acknowledge Sam Key's pioneering effort in developing a JAS3D strategy for dealing with nearly incompressible material behavior.

Contents

Figures

Tables

1. Introduction

The "Rheology of Green Carbon Black-Filled Rubber" has been summarized by D. B. Adolf in a Sandia report [1]. Adolf found that the predictions from a separable K-BKZ constitutive equation seemed to provide reasonable agreement with experimental data obtained from single step strain, stress relaxation experiments. Although the K-BKZ formalism may be suggested by the experimental data, the formalism poses severe computational hardships which preclude its selection for implementation in a large-scale, three-dimensional finite element code. To circumvent the numerical issues, D. J. Segalman, K. Zuo, and D. Parsons have developed an alternative constitutive equation [2] which is computationally attractive. This report provides documentation for the implementation of their alternative constitutive equation in the JAS3D finite element code.

2. Proposed Constitutive Equation

The proposed constitutive equation makes use of a "damage-like" parameter to account for the apparent strain softening which occurs under deformation. Although this "damage" parameter differs from traditional damage definitions in that it allows healing to occur, I shall avoid the temptation to rename this quantity "Danage" after its "father", Dan Segalman, as suggested by D. B. Adolf.

The finite element implementation of the viscoelastic constitutive equation for rubber is nearly incompressible. However, because there is a finite bulk modulus, the stress and strain tensors are assumed to be partitioned into deviatoric components, $\underset{\sim}{s}$ and $\underset{\sim}{e}$, respectively. The constitutive equation for the deviatoric stress is expressed in a rate form consistent with the superposition of Maxwell models so that

$$\underset{\sim}{s}(t) = \sum_{i=1}^{M} \underset{\sim}{s}_i(t) + 2G_\infty \underset{\sim}{e}(t) \tag{1}$$

Here, the stress is seen to be computed as a sum of "partial" stresses arising from the "M" Maxwell models derived from the "M" terms in the Prony series expansion for the shear stress relaxation modulus, G(t):

$$G(t) = G_\infty + \sum_{i=1}^{M} G_i \exp(-t/\tau_i) \tag{2}$$

The partial stresses evolve according to the governing rate equation:

$$\frac{d\underset{\sim}{s}_i}{dt} + \frac{\underset{\sim}{s}_i}{\tau_i} = 2G_i g(\mathcal{d}) \frac{d\underset{\sim}{e}}{dt} \tag{3}$$

where G_i and τ_i are the shear coefficients and relaxation times from the exponential expansion of the shear relaxation modulus (Equation (2)), and $g(\mathcal{d})$ is a function of the damage parameter, $\mathcal{d}$. The evolution equation for damage is defined to be

$$\frac{d\mathcal{d}}{dt} + \frac{\mathcal{d}}{\lambda_{\mathcal{d}}} = |\underset{\sim}{D}_{\mathcal{d}}| \tag{4}$$

where $\lambda_{\mathcal{d}}$ is the single relaxation time associated with healing of damage and $\underset{\sim}{D}_{\mathcal{d}}$ is a damage strain rate. Notice that the right hand side of Equation 4 is slightly different from the term found in Reference 2. This generalization is consistent with the "current thinking" of Segalman. An L_2 norm is assumed. The damage strain rate is computed by appealing to the definition of a damage surface

$$|\underset{\sim}{e} - \underset{\sim}{e}_K| = e_I \tag{5}$$

where tensor $\underset{\sim}{e}_K$ and scalar e_I are associated with kinematic and isotropic hardening, respectively. The net damage strain rate is defined to be

$$\underset{\sim}{D}_{\mathcal{d}} = \left\{\frac{d\underset{\sim}{e}}{dt} \bullet \underset{\sim}{N}\right\}\underset{\sim}{N} \tag{6}$$

if

$$\frac{d\underset{\sim}{e}}{dt} \bullet \underset{\sim}{N} > 0 \tag{7}$$

and

$$|\underset{\sim}{e} - \underset{\sim}{e}_K| = e_I \tag{8}$$

Otherwise (i.e., when inside the damage surface),

$$\underset{\sim}{D}_{\mathcal{d}} = \underset{\sim}{0} \tag{9}$$

In these equations, $\underset{\sim}{N}$ is the vector defining the outward normal to the damage surface

$$\underset{\sim}{N} = (\underset{\sim}{e} - \underset{\sim}{e}_K)/|\underset{\sim}{e} - \underset{\sim}{e}_K| \tag{10}$$

The evolution equations for $\underset{\sim}{e}_K$ and e_I are

$$\frac{d\underset{\sim}{e}_K}{dt} = (1-\beta)\underset{\sim}{D}_{\mathcal{d}} \tag{11}$$

$$\frac{de_I}{dt} = \beta|\underset{\sim}{D}_{\mathcal{d}}| \tag{12}$$

when

$$|\underset{\sim}{D}_d| > 0 \tag{13}$$

To accommodate healing, the following decay equations must be satisfied:

$$\frac{d\underset{\sim}{e}_K}{dt} = -(\underset{\sim}{e}_K - \underset{\sim}{e})/\lambda_K \tag{14}$$

$$\frac{de_I}{dt} = -e_I/\lambda_I \tag{15}$$

when

$$\underset{\sim}{D}_d = \underset{\sim}{0} \tag{16}$$

β, λ_K, and λ_I are material constants. Notice that in Equation (15), the ε_0 constant from Reference 2 has not been included in the current finite element implementation. This simplification appears to be consistent with our expectations and with the data and fits used for analyses. To ensure that strain states that are within the damage surface are not brought against the damage surface by relaxation processes, the following condition also must be satisfied:

$$\lambda_I \geq \lambda_K \tag{17}$$

2.1 JAS3D Finite Element Implementation

The JAS3D subroutines which evaluate the constitutive equations for the material models are passed the stresses at the beginning of a time step and must output the new stresses at the end of the time step. By convention, the code architecture is set up to compute the Cauchy stress in an unrotated configuration. The typical strain rate adopted for JAS3D constitutive equations is the unrotated deformation rate tensor, $\underset{\sim}{d}$. Although the left stretch, $\underset{\sim}{V}$, and rotation, $\underset{\sim}{R}$, tensors are available within the code for use in constructing other strain measures, a more generalized strain measure has not been utilized in the rubber model largely because there are insufficient large strain data to warrant further investigation. In any event, it is a minor matter to change strain measures should it ultimately become necessary. For the current JAS3D implementation, the following definitions have been employed:

$$\frac{d\underset{\sim}{\varepsilon}}{dt} \equiv \underset{\sim}{d} \tag{18}$$

$$\frac{d\underset{\sim}{e}}{dt} = \underset{\sim}{d} - \underset{\sim}{I}\frac{tr(\underset{\sim}{d})}{3} \tag{19}$$

$$\underset{\sim}{e}(t) = \int_0^t \frac{d\underset{\sim}{e}}{dt} du \tag{20}$$

$$\underset{\sim}{s} = \underset{\sim}{\sigma} - \underset{\sim}{I}\frac{tr(\underset{\sim}{\sigma})}{3} \tag{21}$$

The incremental stress change then can be expressed as

$$\underset{\sim}{\sigma}(t_n) = \underset{\sim}{\sigma}(t_{n-1}) + \Delta\underset{\sim}{s} + \underset{\sim}{I}\frac{tr(\Delta\sigma)}{3} \tag{22}$$

where $\Delta\underset{\sim}{s}$ is the increment in deviatoric stress and the last term is the "pressure" change over the time step. To compute the change in mean stress, an elastic bulk response is assumed so that

$$\frac{\Delta\sigma_{jj}}{3} = K\{\Delta\varepsilon_{jj} - \Delta\Theta\} \tag{23}$$

where K is the bulk modulus, $\Delta\Theta$ is the change in volumetric thermal strain that occurs over the time step, and indicial notation has been employed with repeated subscripts denoting summation.

A further assumption of the rubber model is that the material is thermorheologically simple. This means that all relaxation times (i.e., those from stress relaxation and those from the damage surface and healing) are functions of temperature and scale with a shift factor in logarithm of time so that:

$$\tau_i(T) = a(T)\tau_i(T_{ref}) \tag{24}$$

Equation (24) shows that the relaxation time at temperature T can be obtained from the relaxation time at some reference temperature, T_{ref}, through a multiplicative shift factor, a(T), which is defined by a WLF equation:

$$\log a(T) = \frac{-C_1(T - T_{ref})}{(C_2 + T - T_{ref})} \tag{25}$$

2.2 Integrators for Rate Equations

The rate equations for the deviatoric stress, damage, and damage surface parameters are all first order differential equations of nominally the same form. The strategy for integrating

these equations is a modified central difference algorithm that was developed for a viscoelastic model of glass [3]. The algorithm is summarized below for the deviatoric stress:

$$\underset{\sim}{s}_i(t_n) = \frac{\{2\tau_i(T_{avg}) - \hat{\Delta t}\}}{\{2\tau_i(T_{avg}) + \hat{\Delta t}\}}\underset{\sim}{s}_i(t_{n-1}) + \left\{\frac{4\tau_i(T_{avg})}{2\tau_i(T_{avg}) + \hat{\Delta t}}\right\}G_i g(\dot{d}_{avg})\frac{\Delta \underset{\sim}{e}}{\Delta t_n}(\hat{\Delta t}) \tag{26}$$

where

$$\hat{\Delta t} \equiv \text{MIN}(\Delta t_n, 2\tau_i(T_{avg})) \tag{27}$$

Here, the "avg" subscript denotes the average value over the time step from t_{n-1} to t_n. Using the above algorithm, the change in deviatoric stress over a time step can be evaluated in a form similar to that used in computing an increment of elastic stress:

$$\Delta \underset{\sim}{s} = 2G_{eff}\Delta \underset{\sim}{e} - \underset{\sim}{H} \tag{28}$$

In this equation, the effective shear modulus and the recursive history term are defined by:

$$G_{eff} \equiv G_\infty + \left\{\frac{2g(\dot{d}_{avg})}{\Delta t_n}\right\}\sum_{i=1}^{M}\frac{G_i\tau_i(T_{avg})\hat{\Delta t}}{(2\tau_i(T_{avg}) + \hat{\Delta t})} \tag{29}$$

$$\underset{\sim}{H} \equiv \sum_{i=1}^{M}\left\{\frac{2\hat{\Delta t}}{(2\tau_i(T_{avg}) + \hat{\Delta t})}\right\}\underset{\sim}{s}_i(t_{n-1}) \tag{30}$$

The damage parameter, $\dot{d}$, can be computed in a fashion completely analogous to the deviatoric stress

$$\dot{d}(t_n) = \frac{\{2\lambda_{\dot{d}}(T_{avg}) - \hat{\Delta t}_{\dot{d}}\}}{\{2\lambda_{\dot{d}}(T_{avg}) + \hat{\Delta t}_{\dot{d}}\}}\dot{d}(t_{n-1}) + \left\{\frac{2\lambda_{\dot{d}}(T_{avg})}{2\lambda_{\dot{d}}(T_{avg}) + \hat{\Delta t}_{\dot{d}}}\right\}|\underset{\sim}{D}_{\dot{d}}|(\hat{\Delta t}_{\dot{d}}) \tag{31}$$

where

$$\hat{\Delta t}_{\dot{d}} \equiv \text{MIN}(\Delta t_n, 2\lambda_{\dot{d}}(T_{avg})) \tag{32}$$

The equations for evaluating the drag strain, e_I, and the back strain, $\underset{\sim}{e}_K$, are different depending on whether the damage surface is growing or not. For the particular case when the damage surface is growing, then

$$|\underset{\sim}{D}_{\dot{d}}| > 0 \tag{33}$$

and the drag strain and back strain are computed by

$$e_I(t_n) = e_I(t_{n-1}) + \beta\left|\underset{\sim}{D}_d\right|\Delta t_n \tag{34}$$

$$\underset{\sim}{e}_K(t_n) = \underset{\sim}{e}_K(t_{n-1}) + (1-\beta)\underset{\sim}{D}_d\Delta t_n \tag{35}$$

Otherwise, when healing is underway, then

$$\left|\underset{\sim}{D}_d\right| = 0 \tag{36}$$

and the drag strain and back strain are computed by

$$e_I(t_n) = \frac{\{2\lambda_I(T_{avg}) - \hat{\Delta t}_I\}}{\{2\lambda_I(T_{avg}) + \hat{\Delta t}_I\}} e_I(t_{n-1}) \tag{37}$$

$$\underset{\sim}{e}_K(t_n) = \frac{\{2\lambda_K(T_{avg}) - \hat{\Delta t}_K\}}{\{2\lambda_K(T_{avg}) + \hat{\Delta t}_K\}} \underset{\sim}{e}_K(t_{n-1}) + \left\{\frac{\hat{\Delta t}_K}{2\lambda_K(T_{avg}) + \hat{\Delta t}_K}\right\}\{\underset{\sim}{e}(t_n) + \underset{\sim}{e}(t_{n-1})\} \tag{38}$$

where

$$\hat{\Delta t}_I \equiv \mathrm{MIN}(\Delta t_n, 2\lambda_I(T_{avg})) \tag{39}$$

$$\hat{\Delta t}_K \equiv \mathrm{MIN}(\Delta t_n, 2\lambda_K(T_{avg})) \tag{40}$$

2.3 Nearly Incompressible Behavior

The viscoelastic constitutive equation can be written for an incremental update in terms of a bulk modulus and an effective shear modulus

$$\sigma_{ij}(t_n) = \sigma_{ij}(t_{n-1}) + \{2G_{eff}\Delta e_{ij} - H_{ij}(t_n)\} + \delta_{ij}K\{\Delta\varepsilon_{kk} - \Delta\Theta\} \tag{41}$$

where the second term on the right-hand side is the deviatoric stress increment and the last term is the volumetric (i.e., pressure) increment. When the bulk modulus is much larger than the effective shear modulus, the material becomes "nearly" incompressible. The effective Poisson's ratio, ν_{eff}, is a convenient metric of incompressibility:

$$\nu_{eff} = \frac{3K - 2G_{eff}}{2(3K + G_{eff})} \tag{42}$$

As ν_{eff} approaches 0.5, the material becomes incompressible. Finite element mechanicians have struggled for many years with the numerical hardships involved in modeling nearly incompressible materials as direct solvers are confronted with ill-conditioned matrices and iterative methods must cope with a large spread in eigenvalues. S. W. Key has recently devel-

oped and implemented a multi-level linearization capability within the JAS3D finite element code which has enabled an augmented lagrangian algorithm to obtain solutions to nearly incompressible problems [4]. This approach has already been employed for the nearly incompressible elastic material (i.e., MAT4) in JAS3D. A similar approach has been followed to accommodate the near incompressibility required for the rubber viscoelasticity.

The change in mean stress (hereafter referenced as pressure) is governed by the elastic equation:

$$\Delta P \equiv \frac{\sigma_{kk}(t_n)}{3} - \frac{\sigma_{kk}(t_{n-1})}{3} = K\{\Delta\varepsilon_{kk} - \Delta\Theta\} \tag{43}$$

From this relation, the mechanical volume strain can be obtained in terms of the applied pressure:

$$\{\Delta\varepsilon_{kk} - \Delta\Theta\} = \frac{\Delta P}{K} \tag{44}$$

The finite element solution for nearly incompressible behavior is obtained by solving a sequence of $\{j = 1, 2, \ldots M\}$ "better conditioned" model problems. From the sequence of solutions to these model problems, the pressure is built up incrementally using a softer bulk modulus to reduce the effective Poisson's ratio and acquire a more numerically tractable system of equations. A convenient way of scaling the bulk modulus is to specify a limit on the maximum value of the effective Poisson's ratio, say ν_{max}. Then a softer bulk modulus can be defined by simply scaling the actual bulk modulus by a factor, α so that

$$K_{soft} = \alpha K \tag{45}$$

where

$$\alpha = \frac{2G_{eff}(1 + \nu_{max})}{3K(1 - 2\nu_{max})} \tag{46}$$

The pressure change, ΔP, in the model problems is then evaluated as follows

$$\Delta P = \Delta p_j + (\alpha K)\left\{(\Delta\varepsilon_{kk} - \Delta\Theta) - \frac{\Delta p_j}{K}\right\} \tag{47}$$

where Δp_j is the pressure increment obtained from the solution to the previous model problem. As each model problem solution is obtained, the pressure increment is updated:

$$\Delta p_{j+1} = \Delta p_j(1 - \alpha) + \alpha K\{\Delta\varepsilon_{kk} - \Delta\Theta\} \tag{48}$$

In the limit as the sequence of model problems progresses, the change in the mechanical volume strain, $\Delta\varepsilon_{vol}$, diminishes:

$$\Delta\varepsilon_{vol} \equiv \left\{ (\Delta\varepsilon_{kk} - \Delta\Theta) - \frac{\Delta p_j}{K} \right\} \rightarrow 0 \tag{49}$$

which implies that

$$\Delta P \rightarrow \Delta p_j \rightarrow K\{\Delta\varepsilon_{kk} - \Delta\Theta\} \tag{50}$$

Hence, Equation (43) is ultimately satisfied. Within the context of the finite element code implementation, a convergence criteria must be established for the sequence of model problems. This criteria is based on the L_∞ norm computed with respect to some user specified reference strain, ε_{ref}, so that convergence is achieved when the maximum relative volume strain change is less than some acceptable tolerance:

$$\text{MAX}\left(\frac{\Delta\varepsilon_{vol}}{\varepsilon_{ref}}\right) < \text{TOLERANCE} \tag{51}$$

where the maximum is taken over all finite elements of that material type.

2.4 Damage Function, $g(\mathcal{d})$

A definition of the damage function, $g(\mathcal{d})$, is needed for the finite element implementation. By evaluating the constitutive equations for a "step" shear strain and comparing the resulting stress equation to the stress equation predicted by the K-BKZ model for an identical loading, the damage function can be related directly to the damping function [5]:

$$g(\mathcal{d}) = h(\mathcal{d}) + \mathcal{d} \cdot h'(\mathcal{d}) \tag{52}$$

Note that the h' in Equation (52) is the first derivative of the damping function. On the basis of the data that Adolf has collected [1], the following functional form has been adopted for the damping function as an explicit function of damage:

$$h(\mathcal{d}) = \frac{A_1}{1 + A_2\mathcal{d}} + A_3 \tag{53}$$

where A_1, A_2, and A_3 are constants that must be input by the user as part of the material input definitions. Note that the constants A_1 and A_3 must sum to 1.0 in order for the damping function to be 1.0 when there is zero damage. By adopting the form of Equation (53) for the damping function, Equation (52) can be rewritten in terms of $h(\mathcal{d})$ only:

$$g(\mathcal{d}) = h(\mathcal{d}) - \left\{\frac{A_2}{A_1}\right\}\mathcal{d}\{h(\mathcal{d}) - A_3\}^2 \tag{54}$$

A plot of the damage function, g($\mathcal{d}$) as determined for compounds A and B [1] from a fit of the damping function, h($\mathcal{d}$) is shown in Figure 1. For a single "step" shear strain experiment, the

BEGIN CRADA PROTECTION

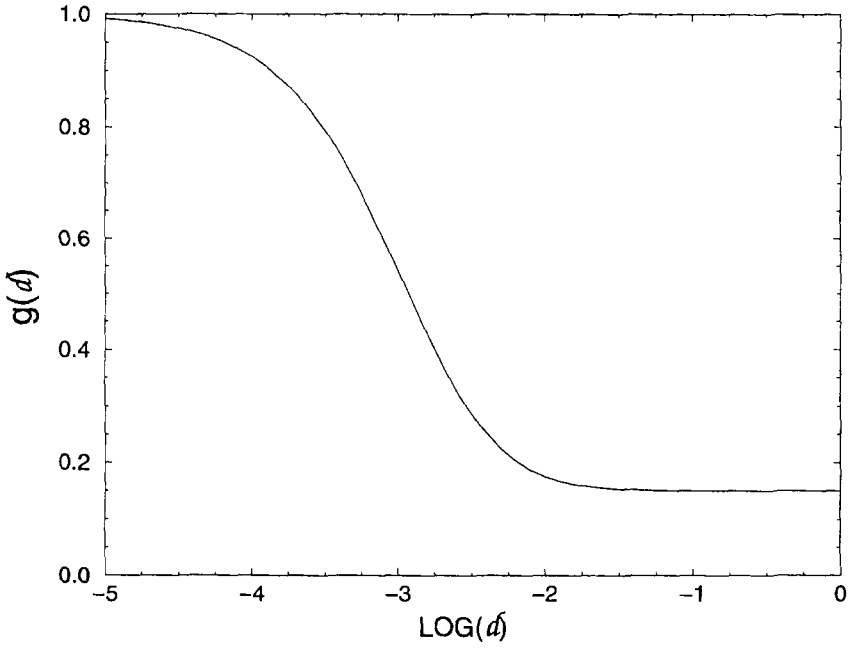

Figure 1. Plot of Damage Function for Compounds A and B

END CRADA PROTECTION

damage, $\mathcal{d}$, can be directly related to the norm of the strain tensor:

$$\mathcal{d} = |\underset{\sim}{e}| \tag{55}$$

3. Example Problems

To demonstrate the performance of the material model, three sets of problems were analyzed: 1) stress relaxation following single "step" strains, 2) stress relaxation following double "step" strains, and 3) cyclic pressurization of a rubber strip. The first two problems were analyzed and compared to experimental data collected by D. Adolf and reported in references 1 and 2. The third problem was included as an illustrative example of how the model behaves. The temperature for all analyses was assumed to be 30°C. The JAS3D input definitions for the viscoelastic rubber material model are provided in APPENDIX A, and the state variables employed in the model are defined in APPENDIX B.

3.1 Stress Relaxation Following Single "Step" Strains

The original data for the damping function was obtained from single "step" strain experiments in which a shear strain was imposed as quickly as physically practical and the subsequent decay in stress was measured. Although the test is described as a "step" strain experiment, the strain is really applied as a rapid ramp. Since the finite element code must prescribe an actual

BEGIN CRADA PROTECTION

Table 1. Material Properties for Filled, Green Rubber

		i	G_i (dynes/cm^2)	τ_i (sec)
C_1 WLF COEF	6.6	1	1.7563E+07	3.0637E-02
C_2 WLF COEF (°C)	150	2	2.1123E+07	2.7725E-01
T_{ref} (°C)	25	3	2.1200E+07	2.3679E+00
β	1	4	1.7805E+07	2.1083E+01
λ_I (sec)	14080	5	1.2748E+07	2.1694E+02
λ_K (sec)	14080	6	7.9129E+06	2.9641E+03
λ_D (sec)	14080	7	4.2505E+06	6.9033E+04
K (dynes/cm^2)	3.22E+10	8	2.1970E+06	6.4199E+06
ν_{max}	0.49			
ε_{ref}	0.0001			
A_1	0.85			
A_2	471.4			
A_3	0.15			
G_∞ (dynes/cm^2)	0.0			

END CRADA PROTECTION

ramp, the period of loading was assumed to be about 0.1 seconds. A list of the material property values input into the JAS3D finite element code is provided in Table 1. Figure 2 contains a comparison between the computed and measured values of the decaying shear relaxation modulus for several different strain amplitudes. The 25% data was obtained and converted from the results of a Goodyear tensile test. The agreement is quite good.

3.2 Stress Relaxation Following Double "Step" Strains

The four double "step" shear strain experiments reported in references 1 and 2 also have been analyzed. For the finite element damage modeling, the "healing" relaxation times (i.e., λ_I, λ_K, and λ_d) were reduced to a value of 200 seconds to match the values used in the analyses found in reference 2. Aside from this change, the material inputs were identical to those defined in Table 1. The four double strain "steps" were:

1. 0.5%, 10 second delay, -1.0%
2. 1.0%, 10 second delay, -1.0%
3. 1.0%, 100 second delay, 1.0%
4. 2.0%, 100 second delay, -0.5%

BEGIN CRADA PROTECTION

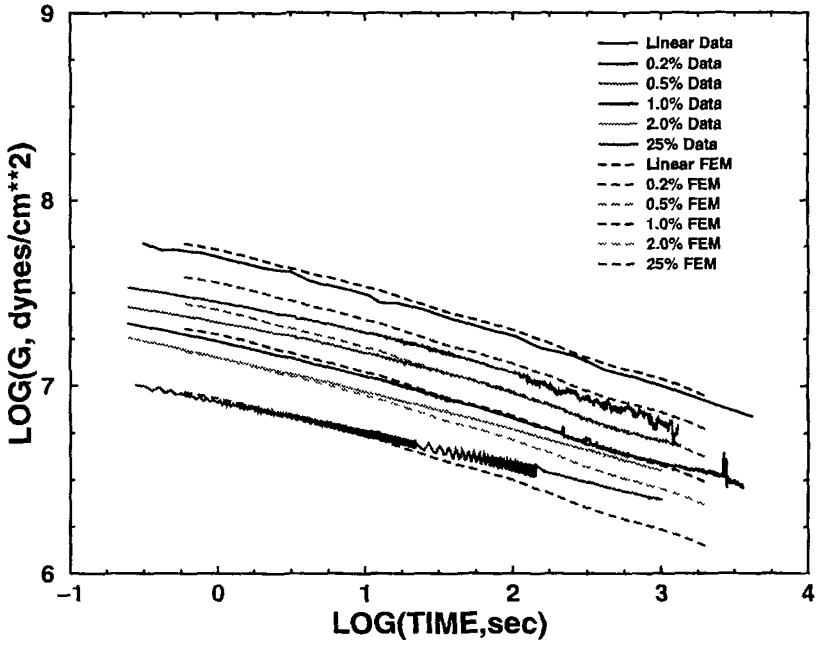

Figure 2. Comparison Between Measured Shear Relaxation Modulus and Finite Element Model Predictions for Various Strain Amplitudes in Single Step Shear Strain Experiments

END CRADA PROTECTION

The above notation denotes the initial strain, the ensuing time delay before applying the second strain, and finally the magnitude of the second strain. The second strain magnitude is specified as a relative strain (i.e., strain relative to the configuration attained following the imposition of the first strain). This means that in case 1 the total strain after the second step has been applied is actually -0.5%. In the finite element analyses, all strains were assumed to be ramped over a time period of 0.1 seconds. Hence, contrary to the simplifications that were made in the constitutive equations evaluated in reference 2 to obtain a solution to a mathematically pure step strain, the finite element analyses were based on finite ramps. The resulting stress histories predicted by the finite element damage model for cases 1-4 are shown in Figures 3-6, respectively. In these figures, the linear viscoelastic responses, the K-BKZ predictions, and the data obtained from the Adolf experiments [1] also are plotted for comparison. Note that the entire computed stress history is plotted including the rise in stress generated by both ramps and holds. Data are shown only for the relaxation following the second strain step. A pronounced difference is seen between the nonlinear and linear predictions due to the apparent "softening" created by straining. The agreement between damage predictions and data is less favorable in the double step strain experiments than it was in the single step strain tests. Double step strain is a much more rigorous test of the model. The fact that this correlation is not as good as the results reported in reference 2 is most likely due to the difference in loading rates (i.e., true step strain versus finite ramp). However, it is also worth mentioning that Equation (4) is slightly different than the corresponding equation reported in reference 2.

BEGIN CRADA PROTECTION

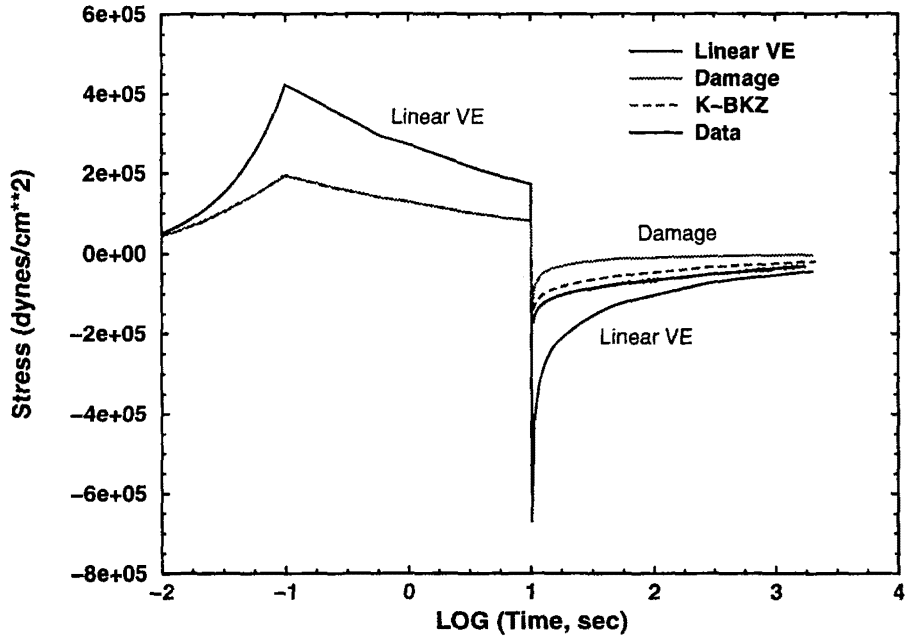

Figure 3. Finite Element Predictions and Data Obtained from Double Step Shear Strain Experiment: (0.5%, 10sec, -1.0%)

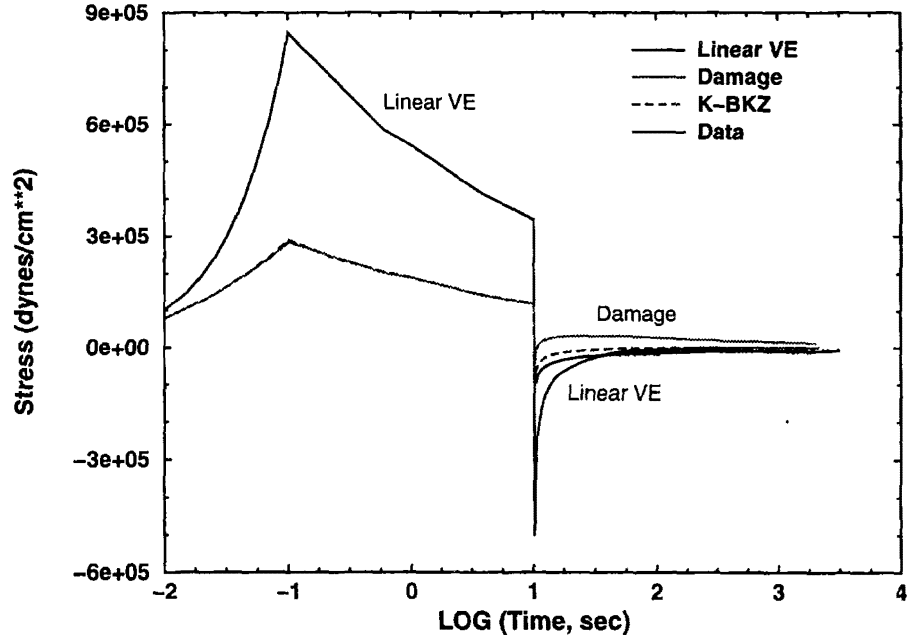

Figure 4. Finite Element Predictions and Data Obtained from Double Step Shear Strain Experiment: (1.0%, 10sec, -1.0%)

END CRADA PROTECTION

BEGIN CRADA PROTECTION

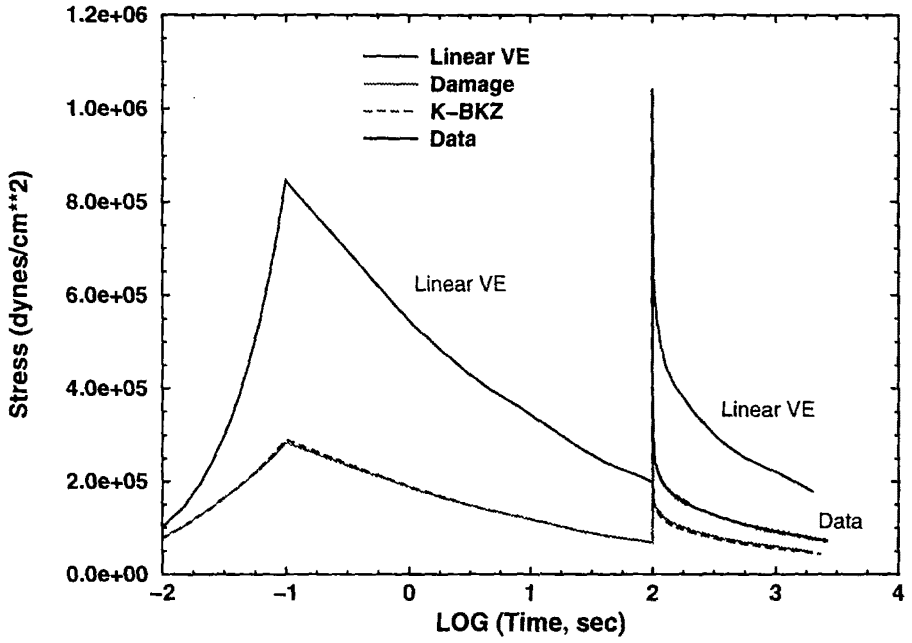

Figure 5. Finite Element Predictions and Data Obtained from Double Step Shear Strain Experiment: (1.0%, 100sec, 1.0%)

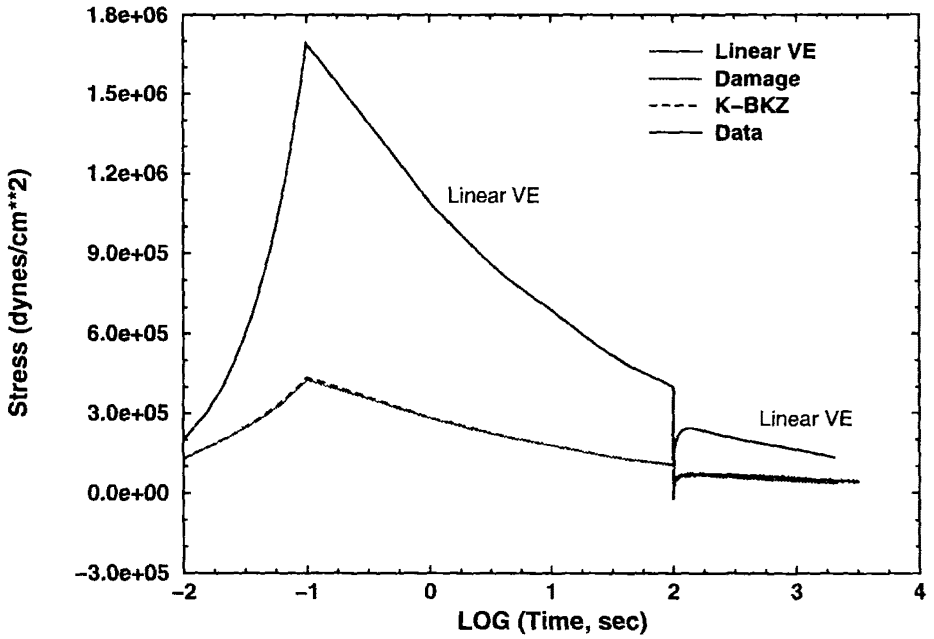

Figure 6. Finite Element Predictions and Data Obtained from Double Step Shear Strain Experiment: (2.0%, 100sec, -0.5%)

END CRADA PROTECTION

It is also known that healing is not governed by a single relaxation time. In fact, a spectrum of relaxation times is needed to capture the observed behavior. This is an added enhancement that affects these results and should be considered for future development.

3.3 Cyclic Pressurization of a Rubber Strip

The final example involves the cyclic pressurization of a rubber strip. The basic geometry and boundary conditions for the problem are depicted in Figure 7. A rubber strip 25 cm long, 2 cm

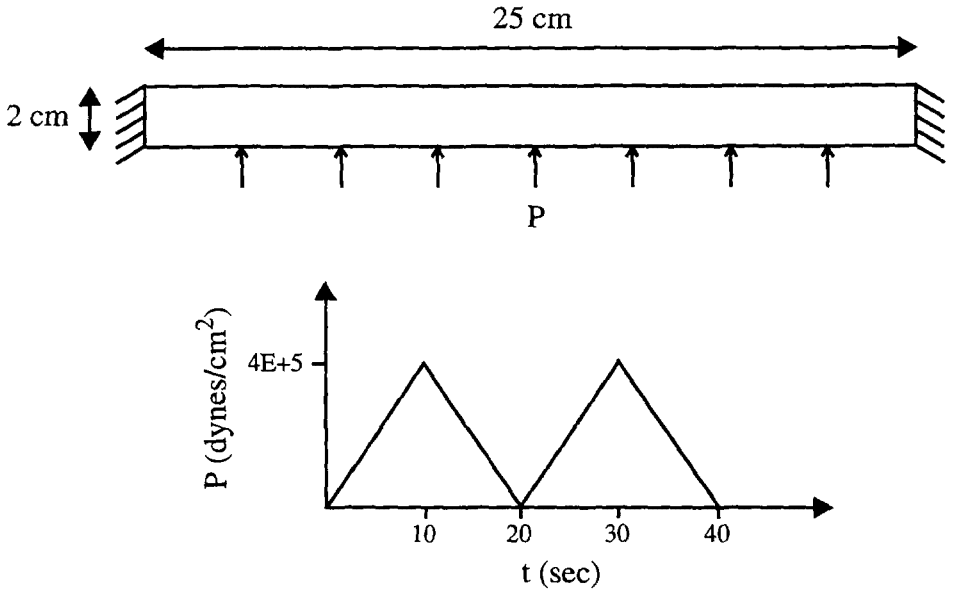

Figure 7. Geometry and Boundary Conditions for Analysis of Rubber Strip Subjected to Cyclic Pressurization

high, and 1 cm thick is clamped at the ends and subjected to a cyclic pressure load as noted in the figure. The maximum applied pressure (4.0E+5 dynes/cm^2) is applied and removed in ramps of 10 seconds. The material properties for this analysis were assumed to be those reported in Table 1 with the lambda relaxation times reduced to 200 seconds. Contour plots of the maximum principal stress on the deformed mesh at times of 10 seconds (max pressure) and 20 seconds (after first unloading) are shown in Figure 8 and Figure 9. As seen in these figures, the rubber strip undergoes substantial deformations. The deformed shape with zero pressure at 20 seconds into the cycle arises from the viscoelastic residual stresses generated by the cyclic loading and the unloading under a reduced (i.e., "damaged") shear modulus. A plot of the damage generated after the first load cycle is shown in Figure 10. The maximum damage is attained at the time of maximum load when the strains are greatest. For the deformations shown in Figure 8, the maximum bending strains (ε_x and ε_z) are 20-25% and the maximum x-y shear strain is 31%. At this level of damage, the material has reached the lower plateau in Figure 1 where $g(d)$ is about 0.15. A time history plot of the maximum deflection at the center of the top of the rubber strip is shown in Figure 11. The ratchet-like behavior results from a combination of viscoelasticity and damage. Although the deformation cycle begins with the stiffness of the full shear modulus, the material quickly attains damage. Hence, the viscoelasticity during the subsequent unloading and reloading is performed under the influence of a

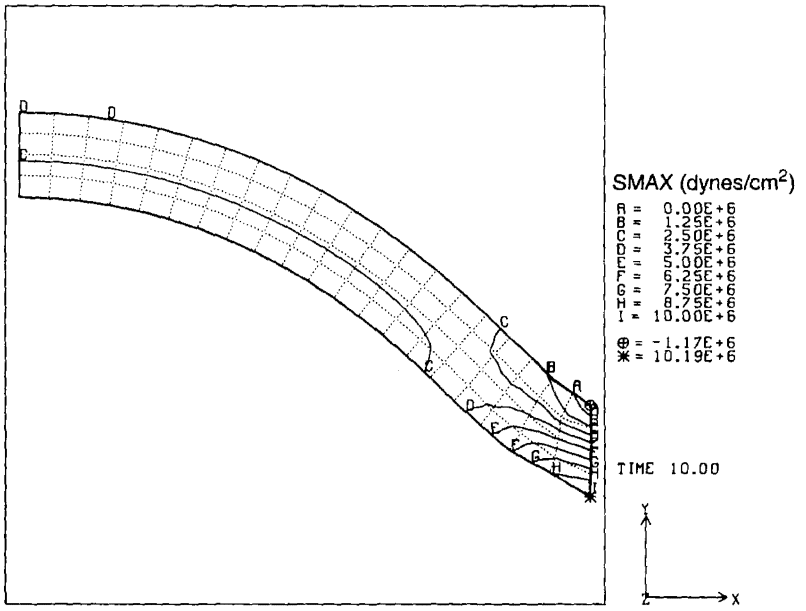

Figure 8. Contour Plot of Maximum Principal Stresses on Deformed Mesh at 10 Seconds into the Pressure Cycle

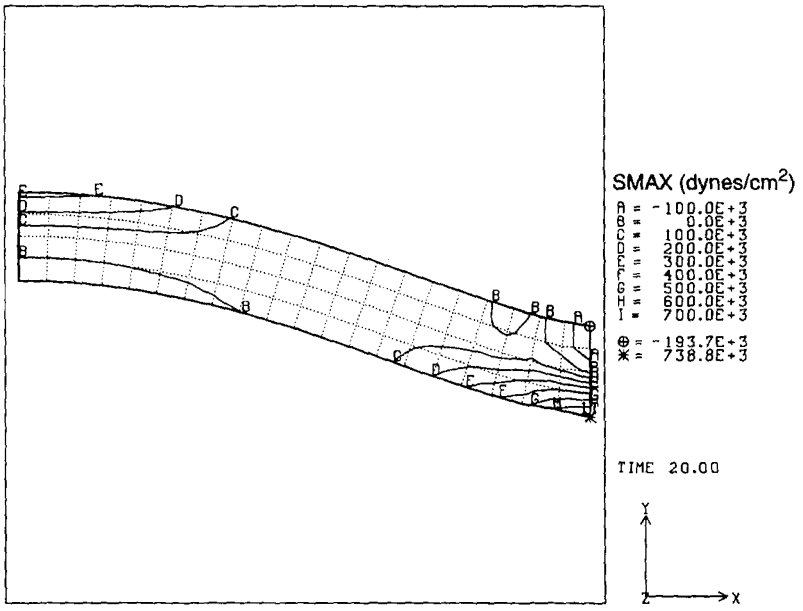

Figure 9. Contour Plot of Maximum Principal Stresses on Deformed Mesh at 20 Seconds into the Pressure Cycle

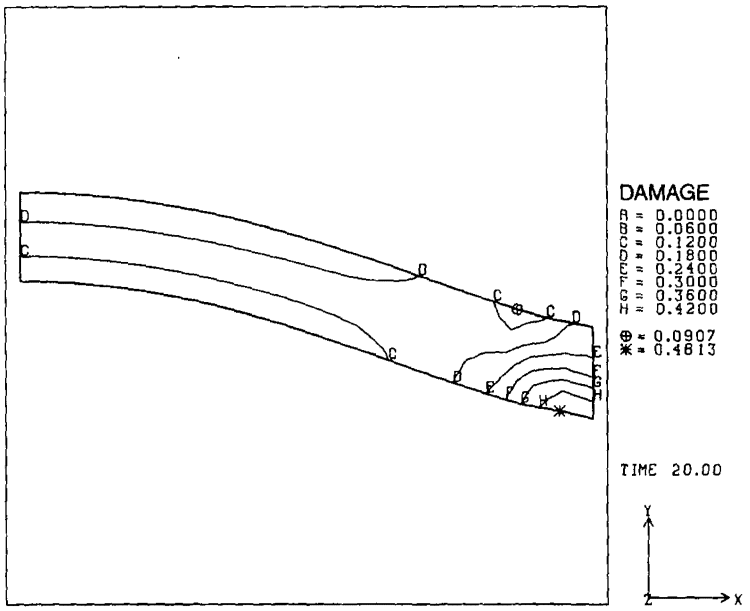

Figure 10. Contour Plot of Damage Parameter at 20 Seconds into the Pressure Cycle (After First Unloading)

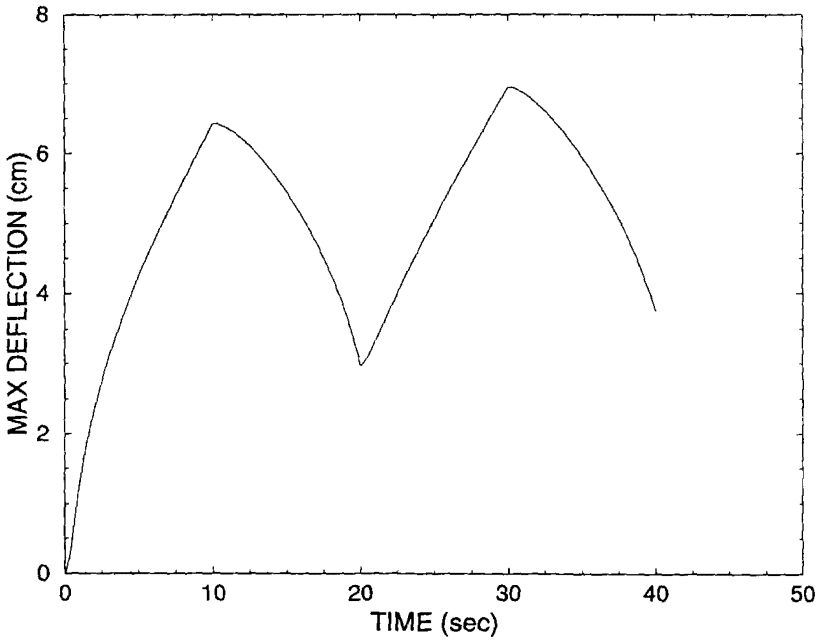

Figure 11. Time History of Maximum Deflection at Center of the Rubber Strip

"reduced" (i.e., in K-BKZ terminology it would be called "damped") shear modulus. The resulting load deflection response for the beam can be seen in the pressure-deflection plot found in Figure 12.

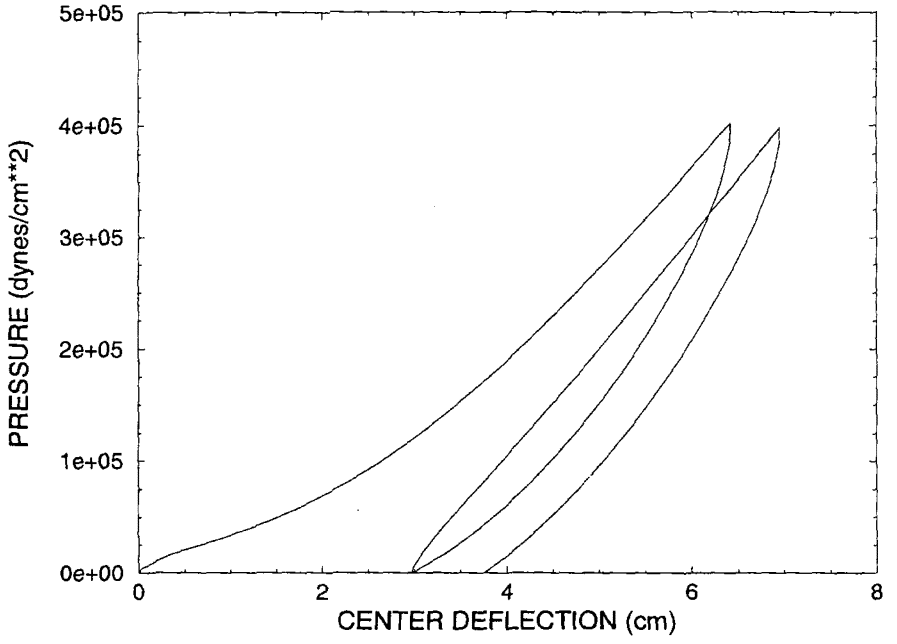

Figure 12. Pressure-Deflection History in Rubber Strip

4. Summary

A version of the D. J. Segalman, K. Zuo, and D. Parsons damage model has been added to the JAS3D finite element code. Single and double "step" shear strain experiments have been analyzed and the model predictions have been compared to experimental results. As expected the correlation for the single step tests is better than that found in the double step strain experiments. A possible improvement could be obtained by adding a spectrum of relaxation times to govern the healing of the damage function. At present, healing is governed by only a single relaxation time. The data seems to require a broader fit.

Another logical extension of this work would be the extensions of the model to encompass the green-to-cure behavior [5].

5. References

1 Adolf, Douglas, "Rheology of Green Carbon Black-Filled Rubber", Sandia National Laboratories, Albuquerque, NM, SAND95-1501, July 1995.

2 Segalman, Daniel J., Zuo, Ken, and Dave Parsons, "Damage, Healing, Molecular Theory, and Modelling of Rubbery Polymer with Active Filler", Sandia National Laboratories, Albuquerque, NM, SAND95-2088, September 1995.

3 Chambers, Robert S., "The Numerical Integration and 3-D Finite Element Formulation of a Viscoelastic Model of Glass", Sandia National Laboratories, Albuquerque, NM, SAND94-1607, August 1994.

4 S. W. Key, Personal Communication.

5 Adolf, Douglas, "Rheology of Carbon-Black Filled Rubber During Cure", Sandia National Laboratories, Albuquerque, NM, SAND96-XXX, to be published.

APPENDIX A

JAS3D Inputs for VISCOELASTIC RUBBER Model

Material Type 30: Viscoelastic Rubber

C1 WLF COEF, C_1
C2 WLF COEF, C_2
WLF REF TEMP, T_{ref}
BETA, β
REF VOL STRAIN, ε_{ref}
I LAMBDA, λ_I
K LAMBDA, λ_K
D LAMBDA, λ_D
BULK MODULUS, K
MAX POISSONS RATIO, ν
A1 DAMP COEF, A_1
A2 DAMP COEF, A_2
A3 DAMP COEF, A_3
RUBBERY SHEAR, G_∞
SHEAR 1, G_1
SHEAR 2, G_2
SHEAR 3, G_3
SHEAR 4, G_4
SHEAR 5, G_5
SHEAR 6, G_6
SHEAR 7, G_7
SHEAR 8, G_8
SHEAR 9, G_9
SHEAR 10, G_{10}
SHEAR RELAX 1, τ_1
SHEAR RELAX 2, τ_2
SHEAR RELAX 3, τ_3
SHEAR RELAX 4, τ_4
SHEAR RELAX 5, τ_5
SHEAR RELAX 6, τ_6
SHEAR RELAX 7, τ_7
SHEAR RELAX 8, τ_8
SHEAR RELAX 9, τ_9
SHEAR RELAX 10, τ_{10}

APPENDIX B

JAS3D State Variables for VISCOELASTIC RUBBER

Material Type 30: Viscoelastic Rubber

VOLEPS, volume strain
AAVG, shift factor $a(T_{avg})$
EPSK1, x component of $\underset{\sim}{e}_K$
EPSK2, y component of $\underset{\sim}{e}_K$
EPSK3, z component of $\underset{\sim}{e}_K$
EPSK4, xy component of $\underset{\sim}{e}_K$
EPSK5, yz component of $\underset{\sim}{e}_K$
EPSK6, zx component of $\underset{\sim}{e}_K$
EPSI, e_I
DAMAGE, D
SDCAYX1, x component of partial stress, $\underset{\sim}{s}_i$, for Prony term i=1
SDCAYY1, y component of partial stress, $\underset{\sim}{s}_i$, for Prony term i=1
SDCAYXY1, xy component of partial stress, $\underset{\sim}{s}_i$, for Prony term i=1
SDCAYYZ1, yz component of partial stress, $\underset{\sim}{s}_i$, for Prony term i=1
SDCAYZX1, zx component of partial stress, $\underset{\sim}{s}_i$, for Prony term i=1
SDCAYX2, x component of partial stress, $\underset{\sim}{s}_i$, for Prony term i=2
SDCAYY2, y component of partial stress, $\underset{\sim}{s}_i$, for Prony term i=2
SDCAYXY2, xy component of partial stress, $\underset{\sim}{s}_i$, for Prony term i=2
SDCAYYZ2, yz component of partial stress, $\underset{\sim}{s}_i$, for Prony term i=2
SDCAYZX2, zx component of partial stress, $\underset{\sim}{s}_i$, for Prony term i=2
. . .
. . .
. . .
SDCAYXi, x component of partial stress, $\underset{\sim}{s}_i$, for Prony term i
SDCAYYi, y component of partial stress, $\underset{\sim}{s}_i$, for Prony term i
SDCAYXYi, xy component of partial stress, $\underset{\sim}{s}_i$, for Prony term i
SDCAYYZi, yz component of partial stress, $\underset{\sim}{s}_i$, for Prony term i
SDCAYZXi, zx component of partial stress, $\underset{\sim}{s}_i$, for Prony term i
BLKSCALE, bulk modulus scale factor
GOFD, $g(d)$
SHEAREFF, component of effective shear modulus
AUGPRESS, Augmented Lagrange pressure increment

(where i goes up to 10)

Distribution:

1 Loren K. Miller
The Goodyear Tire and Rubber Company
Goodyear Technical Center
P. O. Box 3531
Akron, Ohio 44309-3531

1 Robert L. Benedict
The Goodyear Tire and Rubber Company
Goodyear Technical Center
P. O. Box 3531
Akron, Ohio 44309-3531

5 Ahmet Talug
The Goodyear Tire and Rubber Company
Goodyear Technical Center
P. O. Box 3531
Akron, Ohio 44309-3531

1 Mahmoud Assaad
The Goodyear Tire and Rubber Company
Goodyear Technical Center
P. O. Box 3531
Akron, Ohio 44309-3531

5 Thomas G. Ebbott
The Goodyear Tire and Rubber Company
Goodyear Technical Center
P. O. Box 3531
Akron, Ohio 44309-3531

1 Vladimir Kerchman
The Goodyear Tire and Rubber Company
Goodyear Technical Center
P. O. Box 3531
Akron, Ohio 44309-3531

1 Thomas Fleischman
The Goodyear Tire and Rubber Company
Goodyear Technical Center
P. O. Box 3531
Akron, Ohio 44309-3531

Sandia Internal:

1 MS0333 D. B. Adolf, 1841

1 MS9042 L. Weingarten, 8742

1 MS9042 W. Y. Lu, 8746

1 MS0841 P. J. Hommert, 9100

1	MS0828	A. E. Hodapp, 9117
1	MS0443	H. S. Morgan, 9117
3	MS0443	R. S. Chambers, 9117
1	MS0443	B. J. Thorne, 9117
1	MS0443	M. W. Heinstein, 9117
1	MS0443	S. W. Key, 9117
1	MS0437	R. K. Thomas, 9118
3	MS0439	D. J. Segalman, 9234
1	MS9018	Central Technical Files, 8940-2
5	MS 0899	Technical Library, 4414
2	MS0619	Review & Approval Desk for DOE/OSTI, 12690